Am J Nucl Med Mol Imaging 2023;13(3):95-106
www.ajnmmi.us /ISSN:2160-8407/ajnmmi0151085

Original Article

A carbon-11 labeled imidazo[1,2-*a*]pyridine derivative as a new potential PET probe targeting PI3K/mTOR in cancer

Wenqing Liu[1], Wenjie Ma[1], Min Wang[2], Zhuangzhuang Wang[1], Shaun D Grega[2], Qi-Huang Zheng[2], Zhidong Xu[1]

[1]*College of Chemical & Pharmaceutical Engineering, Key Laboratory of Molecular Chemistry for Medicine of Hebei Province, Hebei University of Science & Technology, Shijiazhuang, Hebei, China;* [2]*Department of Radiology and Imaging Sciences, Indiana University School of Medicine, Indianapolis, IN, USA*

Received May 5, 2023; Accepted May 13, 2023; Epub June 25, 2023; Published June 30, 2023

Abstract: The PI3K/Akt/mTOR pathway is frequently dysregulated in cancer due to its central role in cell growth, survival, and proliferation. Overactivation of the PI3K/Akt/mTOR pathway may occur through varying mechanisms including mutations, gene amplification, and upstream signaling events, ultimately resulting in cancer. Therefore, PI3K/Akt/mTOR pathway has emerged as an attractive target for cancer therapy and imaging. A promising approach to inhibit this pathway involves a simultaneous inhibition of both PI3K and mTOR using a dual inhibitor. Recently, a potent dual PI3K/mTOR inhibitor, 2,4-difluoro-*N*-(2-methoxy-5-(3-(5-(2-(4-methylpiperazin-1-yl)ethyl)-1,3,4-oxadiazol-2-yl)imidazo[1,2-*a*]pyridin-6-yl)pyridin-3-yl)benzenesulfonamide (**7**), was discovered and demonstrated excellent kinase selectivity IC_{50} (PI3K/mTOR) = 0.20/21 nM; good cellular growth inhibition IC_{50} (HCT-116 cell) = 10 nM, modest plasma clearance, and acceptable oral bioavailability. Expanding on this discovery, here we present the synthesis of the carbon-11 labeled imidazo[1,2-*a*]pyridine derivative 2,4-difluoro-*N*-(2-methoxy-5-(3-(5-(2-(4-[^{11}C]methylpiperazin-1-yl)ethyl)-1,3,4-oxadiazol-2-yl)imidazo[1,2-*a*]pyridin-6-yl)pyridin-3-yl)benzenesulfonamide (*N*-[^{11}C]**7**) as a new potential radiotracer for the biomedical imaging technique positron emission tomography (PET) imaging of PI3K/mTOR in cancer. The reference standard **7** and its *N*-demethylated precursor, 2,4-difluoro-*N*-(2-methoxy-5-(3-(5-(2-(piperazin-1-yl)ethyl)-1,3,4-oxadiazol-2-yl)imidazo[1,2-*a*]pyridin-6-yl)pyridin-3-yl)benzenesulfonamide (**11**), were synthesized in 7 and 8 steps with 10% and 7% overall chemical yield, respectively. *N*-[^{11}C]**7** was prepared from **11** using [^{11}C]methyl triflate ([^{11}C]CH_3OTf) through *N*-^{11}C-methylation and isolated by high-performance liquid chromatography (HPLC) and solid-phase extraction (SPE) formulation in 40-50% radiochemical yield decay corrected to end of bombardment (EOB) based on [^{11}C]CO_2. The radiochemical purity was > 99% and the molar activity (A_m) at EOB was in the range of 296-555 GBq/μmol (n = 5).

Keywords: Phosphoinositide 3-kinase (PI3K), mammalian target of rapamycin (mTOR), carbon-11 labeled PI3K/mTOR dual inhibitor, radiosynthesis, positron emission tomography (PET), cancer imaging

Introduction

Phosphoinositide 3-kinase (PI3K), mammalian target of rapamycin (mTOR), and protein kinase B (PKB), also known as (AKA) Akt, are critical signaling molecules involved in the regulation of cellular growth, proliferation, and survival [1-3]. Overactivation of the PI3K/Akt/mTOR signaling pathway is one of the most commonly involved pathways in human cancers through promoting proliferation and simultaneously downregulating apoptosis [4]. For this reason, numerous drugs targeting these signaling molecules have been developed and are currently being evaluated in preclinical and clinical trials including GSK2126458 (GlaxoSmithKline) and Pictilisib, AKA GDC-0941 (Genentech) [5].

As the development of diagnostic imaging agents is akin to that of therapeutic drugs, the PI3K/Akt/mTOR pathway is an appealing target for the innovation of imaging probes [6]. The advanced biomedical imaging technique positron emission tomography (PET) is a promising

molecular imaging modality for PI3K/Akt/mTOR pathway-related diseases, fueling the growing interest to design and evaluate new PET radiotracers for *in vivo* imaging of PI3K/Akt/mTOR pathway [7, 8]. Imaging the PI3K/Akt/mTOR pathway will enable researchers and clinicians to identify patients with potential benefit from pathway inhibitors, monitor treatment progression, and elucidate mechanisms of drug resistance.

However, *in vivo* PET imaging probes currently available for PI3K/Akt/mTOR are limited and non-specific. Only ^{18}F-fluoro-2-deoxy-glucose (^{18}F-FDG) and ^{18}F-fluorothymidine (^{18}F-FLT) have been reported to evaluate early-response biomarkers for PI3K/Akt/mTOR inhibition in a breast cancer model [9, 10]. Hence, there is an urgent need to develop PET probes for imaging the PI3K/Akt/mTOR pathway.

A potential strategy to inhibit and image the PI3K/Akt/mTOR pathway involves utilizing dual PI3K/mTOR inhibitors to simultaneously target multiple connections in the PI3K/Akt/mTOR pathway. In our previous work, we pioneered the synthesis of dual PI3K/mTOR inhibitor radiotracers, namely [^{11}C]GSK2126458 and [^{18}F]GSK2126458 [11], as shown in **Figure 1**. Lan group subsequently synthesized carbon-11 and fluorine-18 labeled Pictilisib (GDC-0941) analogs [12, 13] (**Figure 1**) and evaluated these PET tracers in breast cancer animal models. To date, no clinical evaluation of a PI3K/mTOR PET tracer has been reported. Nevertheless, there remains opportunity for pharmacodynamic and pharmacokinetic improvement. Novel radiolabeled PI3K/mTOR dual inhibitors will exhibit differences in metabolism as well as provide different molecular imaging applications in the diagnosis and treatment of diseases. Therefore, a new radiolabeled PI3K/mTOR dual inhibitor is required in the current study.

In this ongoing study, we synthesized a carbon-11 labeled potent and selective PI3K/mTOR dual inhibitor 2,4-difluoro-*N*-(2-methoxy-5-(3-(5-(2-(4-[^{11}C]methylpiperazin-1-yl)ethyl)-1,3,4-oxadiazol-2-yl)imidazo[1,2-*a*]pyridin-6-yl)pyridin-3-yl)benzenesulfonamide (*N*-[^{11}C]**7**, **Figure 1**) as a new potential PET cancer imaging agent. 2,4-Difluoro-*N*-(2-methoxy-5-(3-(5-(2-(4-methylpiperazin-1-yl)ethyl)-1,3,4-oxadiazol-2-yl)imidazo[1,2-*a*]pyridin-6-yl)pyridin-3-yl)benzenesulfonamide (**7**) is an imidazo[1,2-*a*]pyridine derivative recently developed for use as a cancer therapeutic [14]. This lead compound exhibited excellent kinase selectivity IC_{50} (PI3K/mTOR) = 0.20/21 nM; good cellular growth inhibition IC_{50} (HCT-116 cell) = 10 nM, modest plasma clearance, acceptable oral bioavailability, and has *O*- and *N*-methyl positions amenable to labeling with carbon-11. Therefore, its carbon-11 labeled radiotracer is expected to have high specific binding to PI3K/mTOR. Here we report the design, synthesis, and labeling of *N*-[^{11}C]**7**.

Materials and methods

General

All commercial reagents and solvents were purchased from Sigma-Aldrich and Fisher Scientific and used without further purification. [^{11}C]Methyl triflate ([^{11}C]CH_3OTf) was prepared according to a literature procedure [15]. Melting points were determined on WRR apparatus and were uncorrected. ^{1}H and ^{13}C NMR spectra were recorded on a Bruker Avance II 500 MHz NMR Fourier transform spectrometer at 500 and 125 MHz, respectively. Chemical shifts (δ) are reported in parts per million (ppm) relative to an internal standard tetramethylsilane (TMS, δ 0.0) (^{1}H NMR) and to the solvent signal (^{13}C NMR), and coupling constants (*J*) are reported in hertz (Hz). Liquid chromatography-mass spectra (LC-MS) analysis was performed on Q Exactive Mass Spectrometer from Thermo Scientific, USA, consisting of an 1100 series HPLC connected to a diode array detector and a 1946D mass spectrometer configured for positive-ion/negative-ion electrospray ionization (ESI). The high-resolution mass spectra (HRMS) were obtained using a Waters/Micromass LCT Classic spectrometer. Chromatographic solvent proportions are indicated as volume: volume ratio. Thin-layer chromatography (TLC) was run using HS silica gel GF254 uniplates (5 × 10 cm^2). Plates were visualized under UV light. Normal phase flash column chromatography was carried out on Combiflash Rf 150 silica gel 60 (300-400 mesh) with a forced flow of the indicated solvent system in the proportions described below. All moisture- and air-sensitive reactions were performed under a positive pressure of nitrogen maintained by a direct line from a nitrogen source.

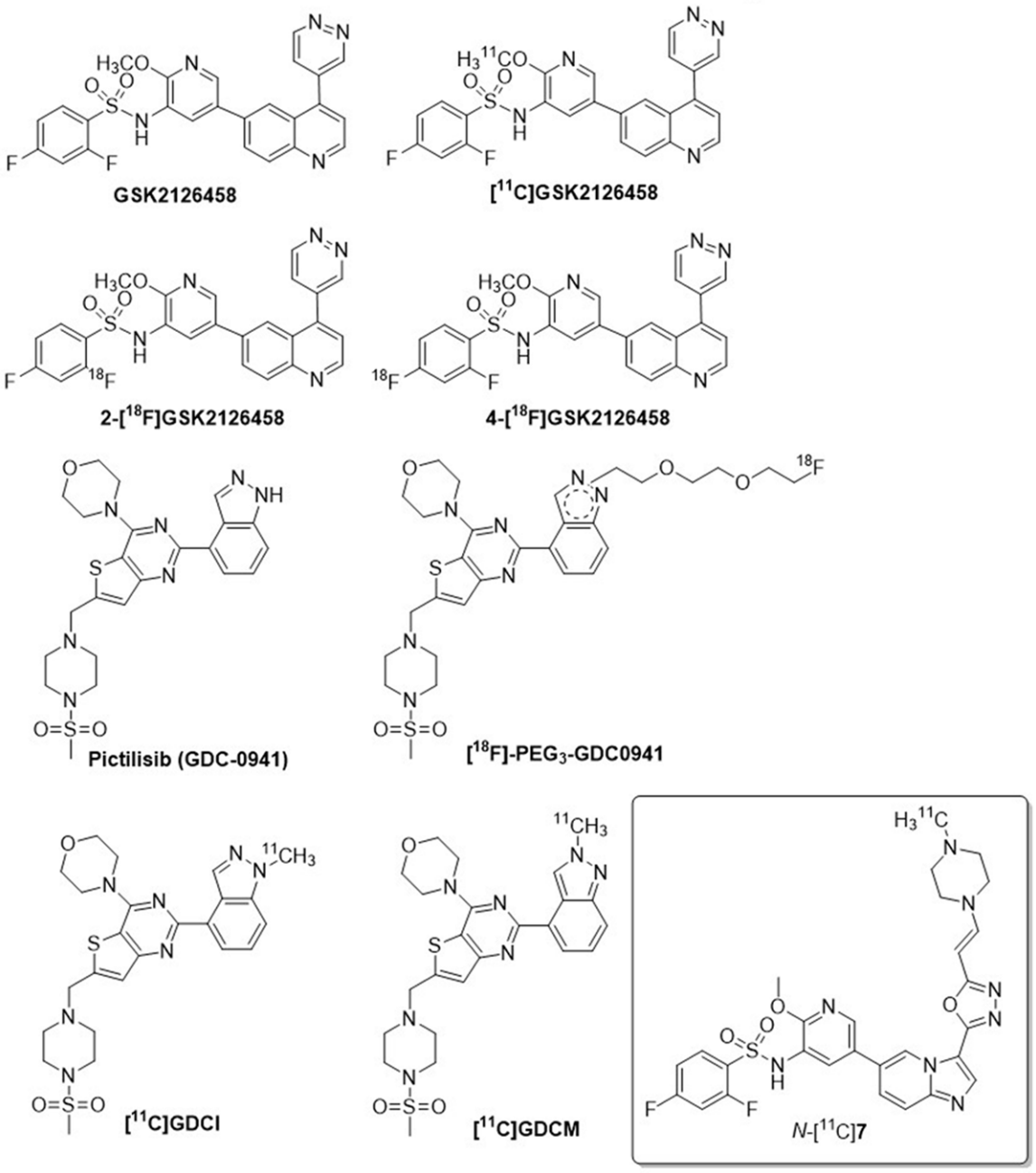

Figure 1. PET PI3K/mTOR probes.

The purity of the synthesized compounds was confirmed by reversed-phase high-performance liquid chromatography (RP-HPLC) using an Agilent Extend 5 TC-C18 column (4.6 × 250 mm, 5 μm) on a Thermo UltiMate 3000 HPLC system, mobile phase 30% CH_3CN/70% 0.1% trifluoroacetic acid (TFA) in water, flow rate 1.0 mL/min and UV (254 nm) flow detector. Analytical RP-HPLC was performed using Waters ACQUITY Arc system, a Prodigy (Phenomenex) 5 μm C-18 column, 4.6 × 250 mm; mobile phase 25% CH_3CN: 75% 20 mM H_3PO_4; flow rate 1.2 mL/min; UV (254 nm) and γ-ray (PIN diode) flow detectors. Semi-preparative RP-HPLC was performed using a Prodigy (Phenomenex) 5 μm C-18 column, 10 × 250 mm; 20% CH_3CN/80% 20 mM H_3PO_4 mobile phase; 5 mL/min flow rate; UV (254 nm) and γ-ray (PIN diode) flow detectors. C18 Plus Sep-Pak cartridges were obtained from Waters

Corporation (Milford, MA). Sterile Millex-FG 0.2 μm filter units were obtained from Millipore Corporation (Bedford, MA).

*Ethyl 6-bromoimidazo[1,2-a]pyridine-3-carboxylate (**1**)*

To a stirred solution of 2-amino-5-bromopyridine (340 mg, 1.95 mmol) in 95% EtOH (10 mL) was added 2-chloro-3-oxopropionic acid ethyl ester (750 mg, 4.98 mmol). The reaction solution was stirred at room temperature (RT) for 1 h, and then stirred for 24 h under reflux. The white solid was removed by filtration, and the filtrate was concentrated under reduced pressure. To the resulting residue, 20 mL of dichloromethane (DCM) was added, and the solution was washed with H_2O (30 mL × 2). The organic layer was dried over anhydrous Na_2SO_4 and filtered. The solvent was removed under vacuum, and the crude product was purified by silica gel column chromatography with petroleum ether/ethyl acetate (10:1) as eluent to afford **1** as a white solid (470 mg, 84%), mp 116.6-117.4°C. ^{1}H NMR (500 MHz, DMSO-d_6): δ 9.34 (d, J = 1.7 Hz, 1H), 8.31 (s, 1H), 7.82 (d, J = 9.5 Hz, 1H), 7.73 (dd, J = 9.5, 1.9 Hz, 1H), 4.38 (q, J = 7.1 Hz, 2H). LC-MS (ESI, *m/z*): Calcd for $C_{10}H_9BrN_2O_2$ ($M+H^+$) 269.0, found: 269.1.

*6-bromoimidazo[1,2-a]pyridine-3-carbohydrazide (**2**)*

To a solution of compound **1** (120 mg, 0.45 mmol) in 95% ethanol (10 mL), hydrazine hydrate (450 mg, 8.92 mmol) was added, the reaction mixture was stirred at reflux for 13 h. The reaction mixture was cooled to RT. The precipitate was collected by filtration and washed with 95% ethanol, and the resulting solid was dried to afford compound **2** as white needle crystals (100 mg, 88%), mp 221.4-222.0°C. ^{1}H NMR (500 MHz, DMSO-d_6): δ 9.87 (s, 1H), 9.61 (d, J = 1.2 Hz, 1H), 8.29 (s, 1H), 7.72 (dd, J = 9.5, 0.7 Hz, 1H), 7.60 (dd, J = 9.5, 2.0 Hz, 1H), 4.52 (s, 1H). LC-MS (ESI, *m/z*): Calcd for $C_8H_7BrN_4O$ ($[M+H]^+$) 256.1, found: 256.9.

*2-(6-bromoimidazo[1,2-a]pyridin-3-yl)-5-vinyl-1,3,4-oxadiazole (**3**)*

To a solution of compound **2** (100 mg, 0.39 mmol) in 10 mL of DCM, two drops of acetic acid and acrolein (66 mg, 1.17 mmol) were added, and the reaction mixture was stirred at RT for 10 h. The reaction mixture was cooled down to 0°C, and then iodosobenzenediacetate (IBD) (118 mg, 0.59 mmol) was added. The reaction mixture was stirred at 0°C for 12 h. The solvent was removed under reduced pressure, and the residue was purified by silica gel column chromatography with petroleum ether/ethyl acetate (10:1) as eluent to afford **3** as a white solid white solid (64 mg, 56%), mp 176.4-177.3°C. ^{1}H NMR (500 MHz, DMSO-d_6): δ 9.42 (s, 1H), 8.49 (s, 1H), 7.88 (d, J = 9.5 Hz, 1H), 7.75 (dd, J = 9.5, 1.7 Hz, 1H), 6.95 (dd, J = 17.6, 11.3 Hz, 1H), 6.42 (d, J = 17.6 Hz, 1H), 6.03 (d, J = 11.3 Hz, 1H). LC-MS (ESI, *m/z*): Calcd for $C_{11}H_7BrN_4O$ ($[M+H]^+$) 292.1, found: 292.9.

*N-(5-bromo-2-methoxypyridin-3-yl)-2,4-difluorobenzenesulfonamide (**4**)*

To a solution of 5-bromo-2-hydroxy-3-nitropyridine (4.0 g, 19.8 mmol) in 40 mL of pyridine, 2,4-difluorobenzenesulfonyl chloride (3.2 mL, 23.8 mmol) was added dropwise at 0°C, the reaction mixture was then warmed up to RT and stirred for 10 h. The reaction was quenched by adding 30 mL of cold water. The precipitate was collected by filtration, washed with water, and dried to afford **4** as a pale pink solid (6.6 g, 88%), mp 161.1-162.0°C. ^{1}H NMR (500 MHz, DMSO-d_6): δ 10.46 (s, 1H), 8.13 (d, J = 2.3 Hz, 1H), 7.81-7.73 (m, 2H), 7.57 (s, 1H), 7.23 (d, J = 2.3 Hz, 1H), 3.61 (s, 3H). LC-MS (ESI, *m/z*): Calcd for $C_{12}H_9BrF_2N_2O_3S$ ($[M+H]^+$) 380.2, found: 380.9.

*2,4-difluoro-N-(2-methoxy-5-(4,4,5,5-tetramethyl-1,3,2-dioxaborolan-2-yl)pyridin-3-yl)benzenesulfonamide (**5**)*

To a solution of compound **4** (200 mg, 0.53 mmol) in 20 mL of anhydrous 1,4-dioxane, bis(pinacolato)diboron (147 mg, 0.58 mmol), $PdCl_2$(dppf)-CH_2Cl_2 (22 mg, 0.026 mmol) and KOAc (155 mg, 3.0 mmol) were add, the reaction flask was purged with nitrogen, and stirred under reflux for 3 h. After the reaction mixture was cooled down to RT, the solid was removed by filtration through celite and washed with DCM and methanol, and the resulting filtrate was concentrated under reduced pressure. The crude product was purified by silica gel column chromatography with petroleum ether/ethyl acetate (10:1) as eluent to afford **5** as a

yellow solid (225 mg, 71%), mp 172.5-173.6°C. ^{1}H NMR (500 MHz, $CDCl_3$): *δ* 8.24 (d, *J* = 1.6 Hz, 1H), 8.02 (d, *J* = 1.6 Hz, 1H), 7.82 (m, 1H), 7.11 (s, 1H), 6.94-6.88 (m, 2H), 3.89 (s, 3H), 1.32 (s, 12H). LC-MS (ESI, *m/z*): Calcd for $C_{18}H_{21}BF_2N_2O_5S$ ([M+Na]$^+$) 449.1, found: 449.1.

*2-(6-bromoimidazo[1,2-a]pyridin-3-yl)-5-(2-(4-methylpiperazin-1-yl)ethyl)-1,3,4-oxadiazole (**6**)*

To a solution of compound **3** (210 mg, 0.72 mmol) in 10 mL of DCM, *N*-methylpiperazine (79 mg, 0.79 mmol) and 1,8-diazabicyclo[5.4.0] undec-7-ene (DBU) (120 mg, 0.79 mmol) were added, and the reaction mixture was stirred at RT for 13 h. The reaction mixture was concentrated under reduced pressure, and the resulting product was purified by silica gel column chromatography with DCM/methanol (50:1) as eluent to afford **6** as a white solid (189 mg, 67%), mp 146.2-147.2°C. ^{1}H NMR (500 MHz, $CDCl_3$): *δ* 9.62 (s, 1H), 8.23 (s, 1H), 7.68 (d, *J* = 9.5 Hz, 1H), 7.51 (dd, *J* = 9.5, 1.5 Hz, 1H), 3.16 (t, *J* = 7.4 Hz, 2H), 2.92 (t, *J* = 7.4 Hz, 2H), 2.60 (s, 4H), 2.45 (s, 4H), 2.29 (s, 3H). LC-MS (ESI, *m/z*): Calcd for $C_{16}H_{19}BrN_6O$ ([M+H]$^+$) 392.3, found: 392.8.

*2,4-difluoro-N-(2-methoxy-5-(3-(5-(2-(4-methylpiperazin-1-yl)ethyl)-1,3,4-oxadiazol-2-yl) imidazo[1,2-a]pyridin-6-yl)pyridin-3-yl)benzenesulfonamide (reference standard, **7**)*

To a solution of compound **6** (200 mg, 0.51 mmol) and compound **5** (240 mg, 0.56 mmol) in 10 mL of 1,4-dioxane and 2 ml of water, potassium carbonate (110 mg, 0.77 mmol) and $PdCl_2$(dppf)-CH_2Cl_2 (37 mg, 0.046 mmol) were added at RT. The reaction mixture was heated and stirred at reflux for 2.5 h with nitrogen protected. After the reaction mixture cooled down to RT, the solid was removed by filtration through celite, and the resulting filtrate was concentrated under reduced pressure. The resulting residue was purified by silica gel column chromatography with DCM/methanol (50:1) as eluent to afford **7** as a white solid (182 mg, 58%), mp 127.1-128.2°C. ^{1}H NMR (500 MHz, $CDCl_3$): *δ* 9.49 (s, 1H), 8.29 (s, 1H), 8.17-8.13 (m, 1H), 8.12 (d, *J* = 1.8 Hz, 1H), 7.99 (d, *J* = 1.8 Hz, 1H), 7.85 (d, *J* = 9.3 Hz, 1H), 7.59 (d, *J* = 9.2 Hz, 1H), 7.27 (dd, *J* = 17.4, 9.5 Hz, 1H), 6.96 (t, *J* = 8.3 Hz, 1H), 3.99 (s, 3H), 3.20 (t, *J* = 7.3 Hz, 2H), 2.95 (t, *J* = 7.4 Hz, 2H), 2.57 (d, *J* = 68.0 Hz, 8H), 2.31 (s, 3H). HRMS (ESI, *m/z*): Calcd for $C_{28}H_{28}F_2N_8O_4S$ ([M-H]$^-$) 609.1850, found: 609.1851.

*2,4-difluoro-N-(2-hydroxy-5-(3-(5-(2-(4-methylpiperazin-1-yl)ethyl)-1,3,4-oxadiazol-2-yl) imidazo[1,2-a]pyridin-6-yl)pyridin-3-yl)benzenesulfonamide (O-demethylated precursor, **8**)*

To a solution of compound **7** (120 mg, 0.20 mmol) in 5 mL of anhydrous acetonitrile, iodotrimethylsilane (79 μL, 0.40 mmol) was added at RT, the reaction mixture was heated and stirred under reflux for 4 h. After the reaction mixture cooled down to RT, the solvent was removed under reduced pressure, and the resulting residue was purified with preparative silica gel TLC to afford **8** as a white solid (96 mg, 82%), mp 158.2-159.3°C. ^{1}H NMR (500 MHz, DMSO-d_6): *δ* 12.34 (s, 1H), 9.27 (s, 1H), 8.36 (s, 1H), 8.04 (t, *J* = 8.5 Hz, 1H), 7.88 (d, *J* = 8.8 Hz, 1H), 7.78 (dd, *J* = 9.4, 1.8 Hz, 1H), 7.69 (s, 2H), 7.56-7.50 (m, 1H), 7.39-7.32 (m, 4H), 7.24-7.21 (m, 2H), 3.07 (dd, *J* = 14.1, 6.9 Hz, 4H), 2.74 (d, *J* = 3.6 Hz, 5H), 2.27 (s, 3H), 1.14 (d, *J* = 7.3 Hz, 3H). HRMS (ESI, *m/z*): Calcd for $C_{28}H_{28}F_2N_8O_4S$ ([M-H]$^-$) 595.1693, found: 595.1698.

*Tert-butyl 4-(2-(5-(6-bromoimidazo[1,2-a] pyridin-3-yl)-1,3,4-oxadiazol-2-yl)ethyl) piperazine-1-carboxylate (**9**)*

To a solution of compound **3** (210 mg, 0.72 mmol) in 10 mL of dichloromethane, *N*-Boc piperazine (79 mg, 0.79 mmol) and DBU (120 mg, 0.79 mmol) were added at RT, the reaction mixture was stirred at RT for 13 h. The solvent was removed under reduced pressure, and the resulting residue was purified by silica gel column chromatography with DCM/methanol (50:1) as eluent to afford **9** as a white solid (192 mg, 68%), mp 144.6-145.6°C. ^{1}H NMR (500 MHz, $CDCl_3$): *δ* 9.62 (s, 1H), 8.24 (s, 1H), 7.68 (d, *J* = 9.5 Hz, 1H), 7.52 (dd, *J* = 9.5, 1.6 Hz, 1H), 3.44 (d, *J* = 4.3 Hz, 4H), 3.18 (t, *J* = 7.2 Hz, 2H), 2.94 (t, *J* = 7.2 Hz, 2H), 2.51 (s, 4H), 1.47 (s, 9H). LC-MS (ESI, *m/z*): Calcd for $C_{20}H_{25}BrN_6O_3$ ([M+H]$^+$) 477.1, found: 477.1.

*Tert-butyl 4-(2-(5-(6-(5-(2,4-difluorophenyl)sulfonamido)-6-methoxypyridin-3-yl) imidazo[1,2-a]pyridin-3-yl)-1,3,4-oxadiazol-2-yl) ethyl)piperazine-1-carboxylate (**10**)*

To a solution of compound **9** (500 mg, 1.05 mmol) and compound **5** (493 mg, 1.16 mmol),

in 10 mL of 1,4-dioxane and 2 mL of H_2O, potassium carbonate (435 mg, 3.15 mmol) and $PdCl_2$(dppf)-CH_2Cl_2 (75 mg, 0.092 mmol) were added. The reaction mixture was stirred at reflex for 3 h under nitrogen protected. After the reaction mixture cooled down to RT, the solid was removed by filtration through celite, and the resulting filtrate was concentrated under reduced pressure. The resulting residue was purified by silica gel column chromatography with DCM/methanol (50:1) as eluent to afford **10** as a white solid (125 mg, 53%), mp 99.8-100.6°C, ^{1}H NMR (500 MHz, $CDCl_3$): *δ* 9.37 (s, 1H), 8.21 (s, 1H), 8.07 (d, *J* = 6.5 Hz, 1H), 8.02 (s, 1H), 7.90 (s, 1H), 7.76 (d, *J* = 9.2 Hz, 1H), 7.52 (d, *J* = 9.2 Hz, 1H), 7.19 (t, *J* = 7.9 Hz, 1H), 6.91 (t, *J* = 8.8 Hz, 1H), 5.24 (s, 1H), 3.89 (s, 3H), 3.39 (s, 4H), 3.16 (t, *J* = 7.1 Hz, 2H), 2.91 (t, *J* = 7.1 Hz, 2H), 2.48 (s, 4H), 1.40 (s, 9H). LC-MS (ESI, *m/z*): Calcd for $C_{32}H_{34}F_2N_8O_6S$ ([M+H]$^+$) 697.2, found: 697.3.

*2,4-difluoro-N-(2-methoxy-5-(3-(5-(2-(piperazin-1-yl)ethyl)-1,3,4-oxadiazol-2-yl)imidazo[1,2-a]pyridin-6-yl)pyridin-3-yl)benzenesulfonamide (N-demethylated precursor, **11**)*

To a solution of compound **10** (500 mg, 0.72 mmol) in 6 mL of dichloromethane, 2 mL of TFA was added dropwise at RT, and the reaction mixture was stirred at RT for 12 h. After removed the solvent under reduced pressure, 20 mL of DI water was added. The pH of the resulting solution was adjusted to 7-8 with 3 N NaOH and extracted with dichloromethane (30 mL × 3). The combined organic layer was washed with 20 mL of saturated brine and 20 mL of water and then dried with anhydrous Na_2SO_4. The organic solvent was removed under reduced pressure, and the resulting product was purified by silica gel column chromatography with DCM/methanol (100:1 to 9:1) as eluent to afford **11** as a white solid (339 mg, 79%), mp 137.0-138.1°C. ^{1}H NMR (500 MHz, DMSO-d_6): *δ* 9.37 (s, 1H), 8.38 (d, *J* = 3.7 Hz, 2H), 7.97-7.92 (m, 2H), 7.92-7.84 (m, 2H), 7.64-7.54 (m, 1H), 7.28 (dd, *J* = 8.5, 2.1 Hz, 1H), 3.73 (s, 3H), 3.22 (t, *J* = 7.0 Hz, 2H), 3.14-3.05 (m, 4H), 2.92 (t, *J* = 7.0 Hz, 2H), 2.73 (s, 4H). ^{13}C NMR (125 MHz, DMSO-d_6): *δ* 164.5, 157.9, 157.5, 146.9, 142.4, 137.8, 132.9, 132.6, 132.5, 127.5, 126.3, 124.7, 124.4, 120.8, 118.3, 112.6, 112.4, 111.4, 106.6, 106.4, 106.2, 54.1, 54.1, 49.5, 43.3, 23.1. HRMS (ESI, *m/z*): Calcd for $C_{27}H_{26}F_2N_8O_4S$ ([M+H]$^+$) 597.1844, found: 597.1844.

*2,4-difluoro-N-(2-methoxy-5-(3-(5-(2-(4-[^{11}C]methylpiperazin-1-yl)ethyl)-1,3,4-oxadiazol-2-yl)imidazo[1,2-a]pyridin-6-yl)pyridin-3-yl)benzenesulfonamide (target tracer, N-[^{11}C]**7**)*

[^{11}C]CO_2 was produced by the ^{14}N(p,α)^{11}C nuclear reaction in the small volume (9.5 cm^3) aluminum gas target provided with the Siemens RDS-111 Eclipse cyclotron. The target gas consisted of 1% oxygen in nitrogen purchased as a specialty gas from Praxair, Indianapolis, IN. Typical irradiations used for the development were 58 μA beam current and 15 min on target. The production run produced approximately 25.9 GBq of [^{11}C]CO_2 at end of bombardment (EOB). *N*-demethylated precursor (**11**, 0.1-0.3 mg) was dissolved in CH_3CN (300 μL). To this solution was added aqueous NaOH (2 N, 2 μL). The mixture was transferred to a small reaction vial. No-carrier-added (high molar activity) [^{11}C]CH_3OTf that was produced by the gas-phase production method [15] within 12 min from [^{11}C]CO_2 through [^{11}C]CH_4 and [^{11}C]CH_3Br with silver triflate (AgOTf) column was passed into the reaction vial at RT until radioactivity reached a maximum (2 min), and then the reaction vial was isolated and heated at 80°C for 3 min. The contents of the reaction vial were diluted with aqueous $NaHCO_3$ (0.1 M, 1 mL). The reaction vial was connected to a 3 mL HPLC injection loop. The labeled product mixture solution was injected onto the semi-preparative HPLC column for purification. The product fraction was collected in a recovery vial containing 30 mL water. The diluted tracer solution was then passed through a C-18 Plus Sep-Pak cartridge and washed with water (3 × 10 mL). The cartridge was eluted with EtOH (3 × 0.4 mL) to release the labeled product, followed by saline (10-11 mL). The eluted product was then sterile-filtered through a Millex-FG 0.2 μm membrane into a sterile vial.

Results and discussion

Chemistry

Synthesis of the reference standard **7** and its *O*-demethylated precursor **8** and *N*-demethylated precursor **11** is depicted in **Figure 2** according to the reported and modified procedures [11, 14, 16-19]. The synthesis of com-

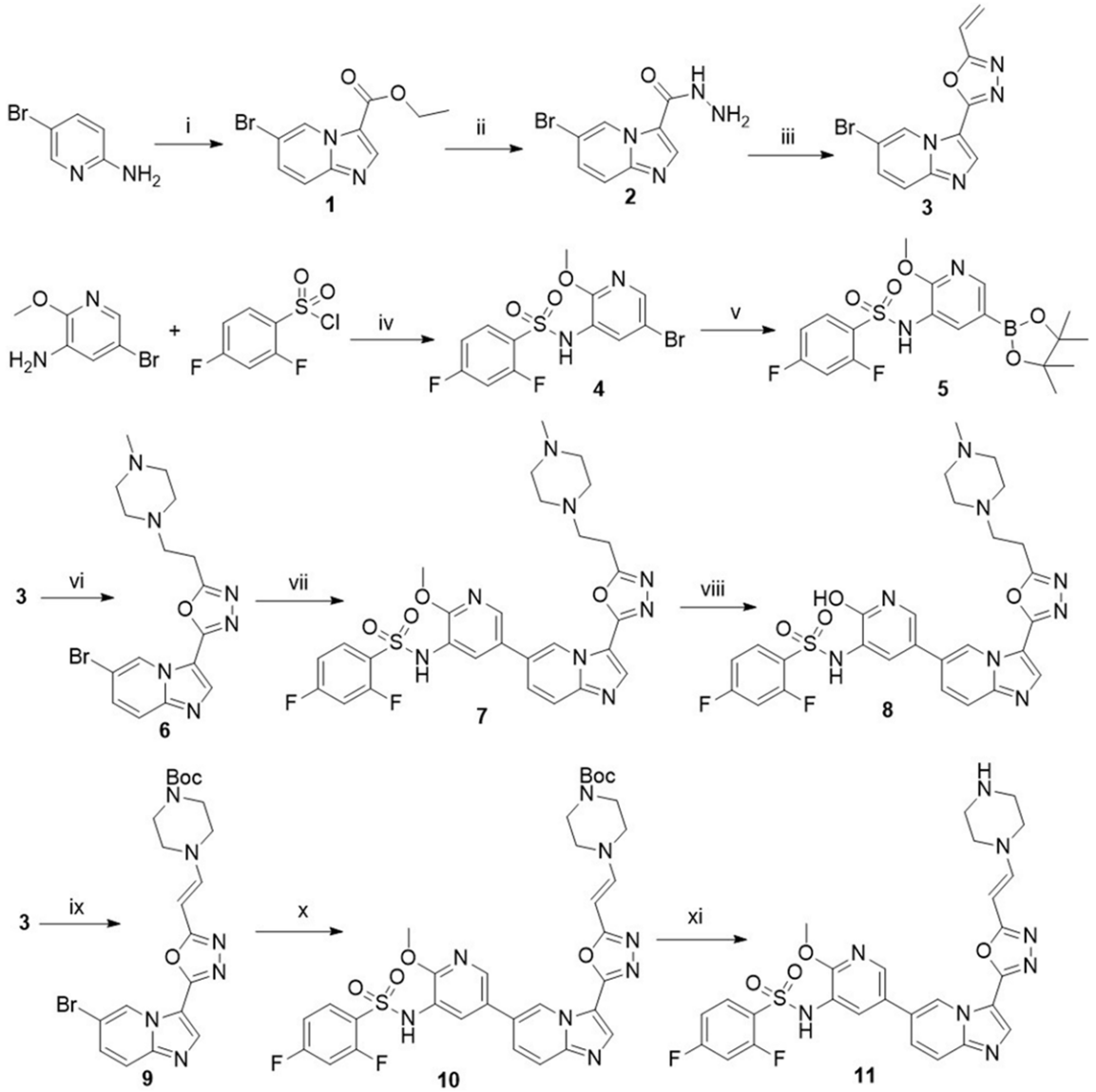

Figure 2. Synthesis of the reference standard **7** and its *O*-demethylated precursor (**8**) and *N*-demethylated precursor (**11**). Reagents and conditions: (i) 2-chloro-3-oxopropionic acid ethyl ester, EtOH, reflux; (ii) hydrazine hydrate, EtOH, reflux; (iii) acrolein, acetic acid, DCM, RT, IBD; (iv) pyridine, RT; (v) bis(pinacolato)diboron, $PdCl_2$(dppf)-CH_2Cl_2, KOAc, 1,4-dioxane, reflux; (vi) *N*-methylpiperazine, DBU, RT; (vii) **5**, K_2CO_3, $PdCl_2$(dppf)-CH_2Cl_2, 1,4-dioxane, reflux; (viii) iodotrimethylsilane, CH_3CN, reflux; (ix) *N*-Boc piperazine, DBU, DCM, RT; (x) **5**, K_2CO_3, $PdCl_2$(dppf)-CH_2Cl_2, 1,4-dioxane, reflux; (xi) TFA, DCM, RT.

pound **1** involved a cyclization reaction between 2-amino-5-bromopyridine and 2-chloro-3-oxopropionic acid ethyl ester following a modified procedure and achieved a yield of 84%. This yield was 24% greater than the reported yield. The hydrazinolysis reaction between compound **1** and hydrazine hydrate in ethanol yielded the intermediate **2** in 88% yield. Hydrazide **2** was treated with acrolein to afford an acyl imine intermediate and then transformed to **3** in 56% yield. Coupling 2,4-difluorobenzenesulfonyl chloride with 5-bromo-2-methoxypyridin-3-amine in pyridine provided compound **4** in 88% yield. Compound **5** was generated *via* a palladium catalyzed cross-coupling reaction of bis(pinacolato)diboron with compound **4** in 71% yield. Compound **6** was prepared from compound **3** via an electrophilic addition with *N*-methylpiperazine in 67% yield. **6** was subsequently engaged in a Suzuki cross-couplings reaction

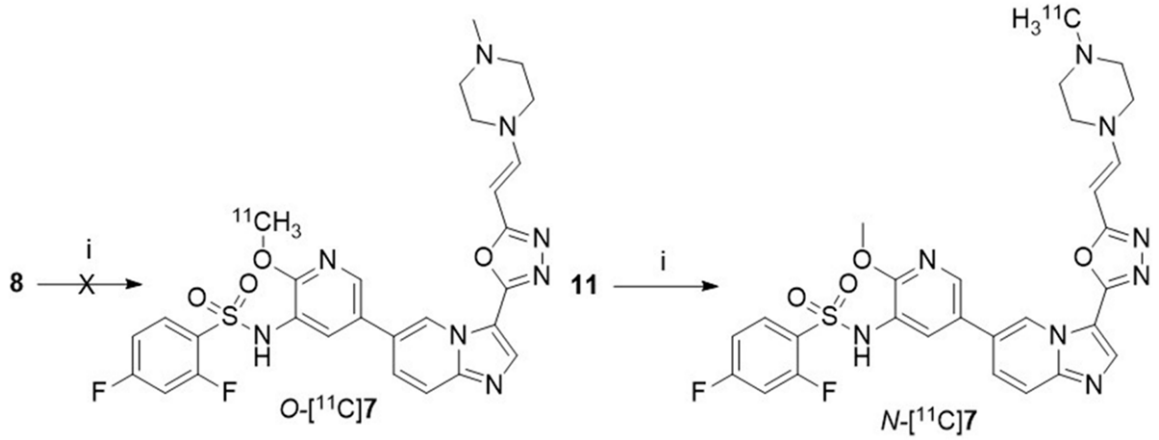

Figure 3. Synthesis of the target radiotracer *N*-[^{11}C]**7**. Reagents and conditions: (i) [^{11}C]CH_3OTf, CH_3CN, 2 N NaOH, 80°C, 3 min.

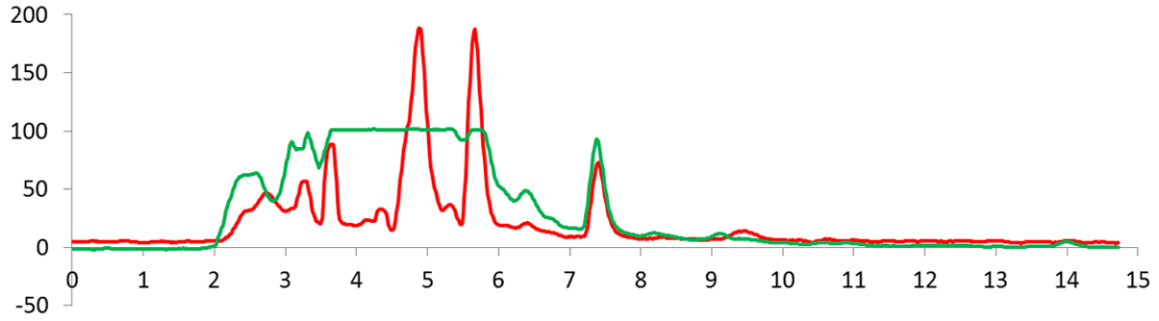

Figure 4. A representative semi-preparative RP-HPLC chromatographic profile for the purification of *O*-[^{11}C]**7**: Red, radioactive HPLC trace; and Green, UV HPLC trace.

with compound **5** to afford compound **7** as the reference standard in 58% yield. The *O*-demethylated precursor **8** was prepared from compound **7** by reacting with iodotrimethylsilane in 82% yield. Compound **3** was subjected to an electrophilic addition with *N*-Boc piperazine to provide intermediate **9** in 68% yield. Compound **10** was prepared from **9** *via* a Suzuki cross-couplings reaction with compound **5** in 53% yield. The *N*-demethylated precursor **11** was prepared from compound **10** by reacting with TFA in dichloromethane in 79% yield.

Radiochemistry

Synthesis of the carbon-11 labeled imidazo[1,2-*a*]pyridine derivative [^{11}C]**7** labeled at both *O*- and *N*-positions is shown in **Figure 3**. *O*-Demethylated precursor **8** underwent *O*-^{11}C-methylation [20, 21] using the reactive ^{11}C-methylating agent [^{11}C]CH_3OTf [15, 22] in acetonitrile at 80°C under basic condition (2 N NaOH) and failed to yield the expected tracer, *O*-[^{11}C]**7**. The different bases including strong, mild, and weak bases were tested in the labeling reaction, but it was still unable to obtain *O*-[^{11}C]**7**. There are many *N*-positions in compound **8**, and the ^{11}C-methylation on *N*-position is a potential competing reaction compared to *O*-position to form ^{11}C-labeled quaternary ammines, rather than *O*-[^{11}C]**7**. A representative semi-preparative RP-HPLC chromatographic profile for purification of *O*-[^{11}C]**7** is shown in **Figure 4**, which shows several polar labeled products, and no relatively lipophilic *O*-[^{11}C]**7** was identified. Similarly, *N*-Demethylated precursor **11** was labeled with [^{11}C]CH_3OTf through *N*-^{11}C-methylation [19, 23] under the same condition to successfully produce the target tracer, *N*-[^{11}C]**7**. The labeled product was isolated by semi-preparative RP-HPLC with a C-18 column and subsequently concentrated by solid-phase extraction (SPE) [11, 24] with a dispos-

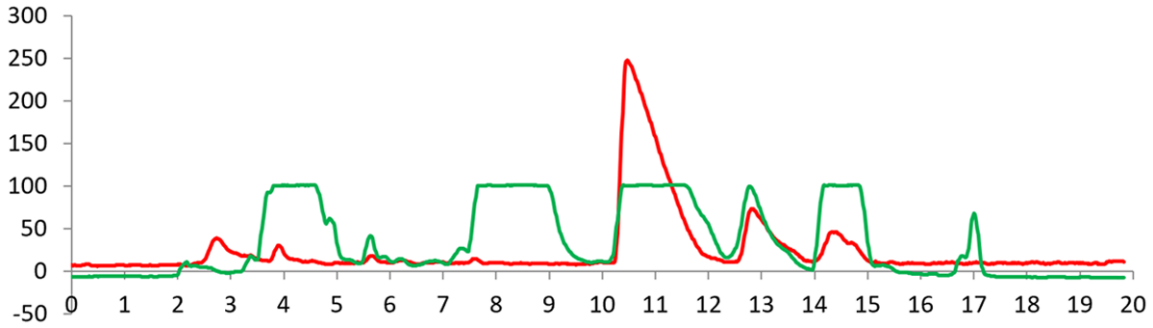

Figure 5. A representative semi-preparative RP-HPLC chromatographic profile for the purification of *N*-[^{11}C]**7**: Red, radioactive HPLC trace; and Green, UV HPLC trace.

able C-18 Plus Sep-Pak cartridge to produce the corresponding pure radiolabeled compound *N*-[^{11}C]**7** in 40-50% radiochemical yield, decay corrected to EOB, based on [^{11}C]CO_2. [^{11}C] Methyl iodide ([^{11}C]CH_3I) is a most commonly used ^{11}C-methylating agent, but [^{11}C]CH_3OTf is more reactive than [^{11}C]CH_3I [15, 21, 22], and thus, the radiochemical yield of *N*-[^{11}C]**7** was relatively high.

Automated radiosynthesis was performed in a self-designed, multi-purpose ^{11}C-radiosynthesis module [25-27]. Our radiosynthesis module facilitated the overall design of the reaction, purification, and reformulation processing, making it suitable for adaptation for human doses. Radiosynthesis included three stages: a labeling reaction, purification, and formulation. In order to prepare the device for subsequent syntheses and minimize radiation exposure to production personnel, automated pre-cleaning routines were employed. Prior to isolation in the hot cell, solvents and/or reagents can be loaded as prompted by the operating software. The overall synthesis time was 35-40 min from EOB. Our module enabled in-process measurement of ^{11}C-tracer molar activity (A_m, GBq/μmol at EOB) using semi-preparative RP-HPLC [25]. At the end of synthesis (EOS), the A_m of ^{11}C-tracer was determined again by analytical RP-HPLC, calculated, and decay-corrected to EOB of [^{11}C]CO_2. Both semi-preparative and analytical RP-HPLC methods gave similar A_m values. The A_m of *N*-[^{11}C]**7** at EOB was in a range of 296-555 GBq/μmol (n = 5). The general method to increase the A_m of ^{11}C-tracer produced in our radiochemistry facility has been studied in our previous work [21]. A representative semi-preparative RP-HPLC chromatographic profile for purification of *N*-[^{11}C]**7** is shown in **Figure 5**.

The radiochemical identity as well as chemical and radiochemical purities were determined by analytical RP-HPLC [28]. **Figure 6** shows a representative chromatographic profile for analysis of *N*-[^{11}C]**7**. The identity of *N*-[^{11}C]**7** was confirmed by comparing the retention time (t_R) to reference standard **7** at 8.919 min (**Figure 6C**). The radioactive HPLC chromatogram (**Figure 6A**) showed the main peak for *N*-[^{11}C]**7** at 9.082 min with > 99% purity. Radiochemical purity was determined through γ-ray (PIN diode) flow detector to be > 99% in all batches. UV HPLC chromatogram (**Figure 6B**) showed a major cold peak at 8.776 min and a few minor cold peaks around 2-3 min, which were identified from the ethanol/saline solution (**Figure 6D**). The peak identification in UV chromatogram was further confirmed by HPLC co-injection [29] of *N*-[^{11}C]**7** with **7** in ethanol/saline solution. Likewise, chemical purity was determined through UV flow detector to be > 99% in all batches. A few identifiable UV peaks from the EtOH/saline used in tracer formulation after HPLC-SPE purification and formulation contributed to minor impurities. However, there is no chemical purity limit for radiotracer release in PET tracer production as radiosynthesis is a micro-scale synthesis resulting in trace amounts of the radiotracer. EtOH, acetonitrile, and acetone were used as cleaning solvents in our ^{11}C-radiosynthesis module. These volatile organic impurities were analyzed and determined by a gas chromatography (GC) equipped with a capillary column and flame ionization detector (FID) to meet all established quality control (QC) criteria. The 1 h

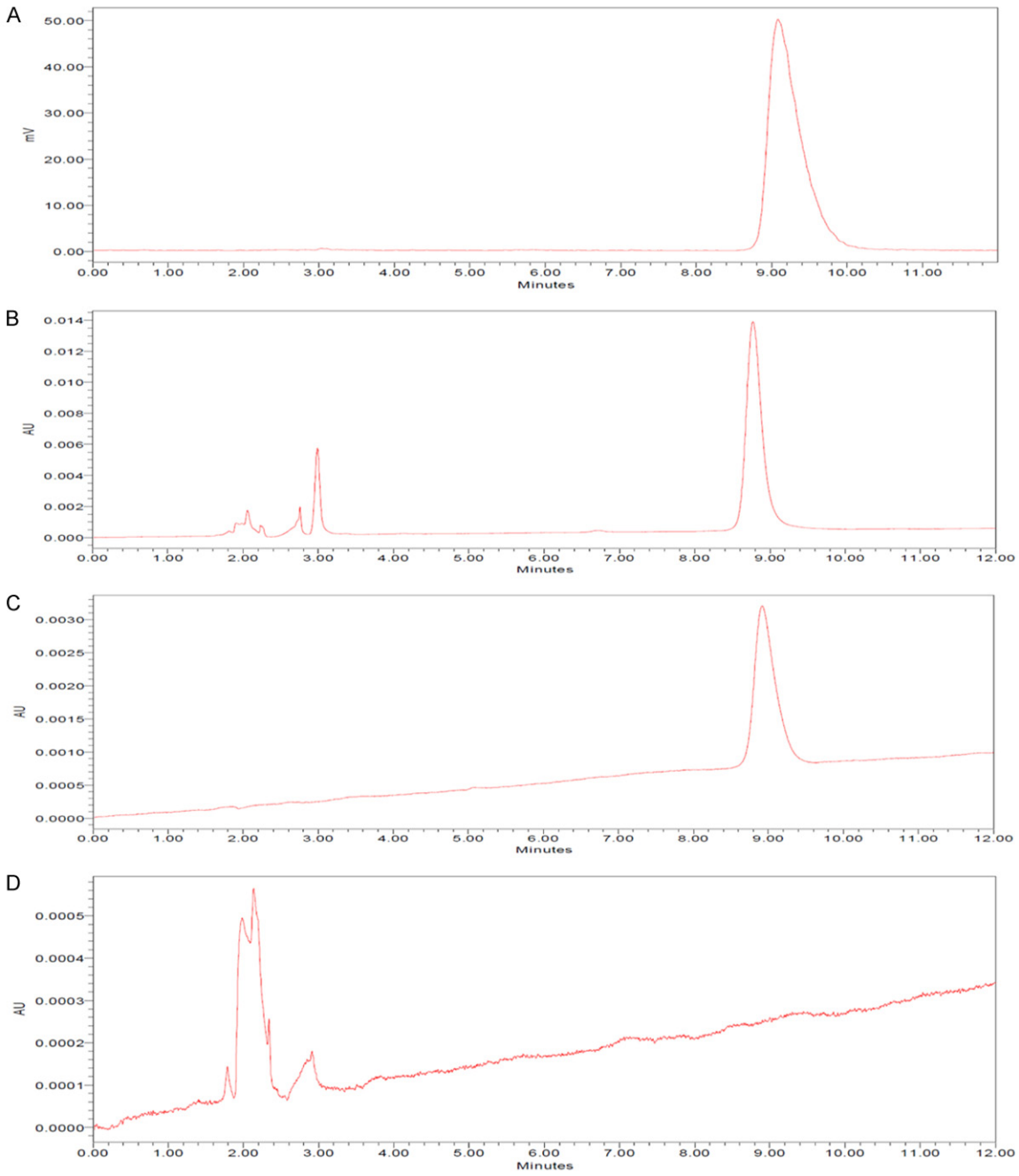

Figure 6. A representative analytical RP-HPLC chromatographic profile for the target tracer's *N*-[^{11}C]**7** radiochemical identity, chemical and radiochemical purity. A: Radioactive chromatogram of *N*-[^{11}C]**7**; B: UV chromatogram of *N*-[^{11}C]**7**; C: UV chromatogram of reference standard **7**; D: UV chromatogram of ethanol in saline.

stability test of the radiotracer after time of terminal sterilizing filtration was performed by analytical HPLC and demonstrated no changes in chemical and radiochemical purity [29], suggesting *N*-[^{11}C]**7** was stable for at least 1 h after terminal sterilizing filtration.

Conclusion

In summary, a multiple step synthetic route with high yields has been developed to produce *O*-demethylated precursor **8**, *N*-demethylated precursor **11**, reference standard **7**, and the

target PET radiotracer, *N*-[^{11}C]**7**. Radiosynthesis utilized [^{11}C]CH_3OTf to carry out *N*-^{11}C-methylation at the piperazinyl nitrogen position of the precursor. The resulting labeled product was subsequently purified by RP-HPLC with a C18 column, followed by SPE with a C18 Plus Sep-Pak cartridge trap/release formulation. *N*-[^{11}C]**7** was obtained in high radiochemical yield, chemical and radiochemical purities, molar activity, and with a reasonably short overall synthesis time. In conclusion, a potent and selective dual PI3K/mTOR inhibitor, labelled with carbon-11, has been successfully radiosynthesized. These results will facilitate future studies to evaluate *N*-[^{11}C]**7** as a new PET agent for the imaging of PI3K/mTOR in cancer and potentially yield novel understandings into this important pathway. The *in vitro* and *in vivo* biological evaluations of *N*-[^{11}C]**7** are currently underway, and the results will be reported in due course.

Acknowledgements

This research was partially supported by the Hebei Province Major Science and Technology Program (No. 17392605D) in China. This work was also partially supported by the Indiana University Department of Radiology and Imaging Sciences in the United States.

Disclosure of conflict of interest

None.

Address correspondence to: Dr. Qi-Huang Zheng, Department of Radiology and Imaging Sciences, Indiana University School of Medicine, 1345 West 16th Street, Room 112, Indianapolis, IN 46202, USA. E-mail: qzheng@iupui.edu; Dr. Zhidong Xu, College of Chemical & Pharmaceutical Engineering, Key Laboratory of Molecular Chemistry for Medicine of Hebei Province, Hebei University of Science & Technology, Shijiazhuang 050018, Hebei, China. E-mail: zdxu@hebust.edu.cn

References

[1] Peng Y, Wang Y, Zhou C, Mei W and Zeng C. PI3K/Akt/mTOR pathway and its role in cancer therapeutics: are we making headway? Front Oncol 2022; 12: 819128.

[2] Mafi S, Mansoori B, Taeb S, Sadeghi H, Abbasi R, Cho WC and Rostamzadeh D. mTOR-mediated regulation of immune responses in cancer and tumor microenvironment. Front Immunol 2021; 12: 774103.

[3] Song M, Bode AM, Dong Z and Lee MH. AKT as a therapeutic target for cancer. Cancer Res 2019; 79: 1019-1031.

[4] Zhu K, Wu Y, He P, Fan Y, Zhong X, Zheng H and Luo T. PI3K/AKT/mTOR-targeted therapy for breast cancer. Cells 2022; 11: 2508.

[5] Wu X, Xu Y, Liang Q, Yang X, Huang J, Wang J, Zhang H and Shi J. Recent advances in dual PI3K/mTOR inhibitors for tumour treatment. Front Pharmacol 2022; 13: 875372.

[6] Agdeppa ED and Spilker ME. A review of imaging agent development. AAPS J 2009; 11: 286-299.

[7] Gaikwad SM and Ray P. Non-invasive imaging of PI3K/Akt/mTOR signalling in cancer. Am J Nucl Med Mol Imaging 2012; 2: 418-431.

[8] Graf N, Li Z, Herrmann K, Weh D, Aichler M, Slawska J, Walch A, Peschel C, Schwaiger M, Buck AK, Dechow T and Keller U. Positron emission tomographic monitoring of dual phosphatidylinositol-3-kinase and mTOR inhibition in anaplastic large cell lymphoma. Onco Targets Ther 2014; 7: 789-798.

[9] Dockx Y, Vangestel C, De Bruycker S, Van den Wyngaert T, Huizing M, Staelens S and Stroobants S. ^{18}F-FDG and ^{18}F-FLT uptake profiles for breast cancer cell lines treated with targeted PI3K/Akt/mTOR therapies. Cancer Biother Radiopharm 2023; 38: 51-61.

[10] Lee M, Minaskan N, Wiedemann T, Irmler M, Beckers J, Yousefi BH, Kaissis G, Braren R, Laitinen I and Pellegata NS. Targeting PI3K/mTOR signaling exerts potent antitumor activity in pheochromocytoma in vivo. Endocr Relat Cancer 2017; 24: 1-15.

[11] Wang M, Gao M, Miller KD, Sledge GW and Zheng QH. [^{11}C]GSK2126458 and [^{18}F]GSK2126458, the first radiosynthesis of new potential PET agents for imaging of PI3K and mTOR in cancers. Bioorg Med Chem Lett 2012; 22: 1569-1574.

[12] Altine B, Gai Y, Han N, Jiang Y, Ji H, Fang H, Niyonkuru A, Bakari KH, Rajab Arnous MM, Liu Q, Zhang Y and Lan X. Preclinical evaluation of a fluorine-18 (^{18}F)-labeled phosphatidylinositol 3-kinase inhibitor for breast cancer imaging. Mol Pharm 2019; 16: 4563-4571.

[13] Han N, Jiang Y, Gai Y, Liu Q, Yuan L, Wang Y, Li M, Zhang Y and Lan X. ^{11}C-labeled pictilisib (GDC-0941) as a molecular tracer targeting phosphatidylinositol 3-kinase (PI3K) for breast cancer imaging. Contrast Media Mol Imaging 2019; 2019: 1760184.

[14] Yu Y, Han Y, Zhang F, Gao Z, Zhu T, Dong S and Ma M. Design, synthesis, and biological evaluation of imidazo[1,2-*a*]pyridine derivatives as

novel PI3K/mTOR dual inhibitors. J Med Chem 2020; 63: 3028-3046.
[15] Mock BH, Mulholland GK and Vavrek MT. Convenient gas phase bromination of [^{11}C]methane and production of [^{11}C]methyl triflate. Nucl Med Biol 1999; 26: 467-471.
[16] Dong CG and Hu QS. Annulative tandem reactions based on $Pd^0/t-Bu_3P$-catalyzed cross-coupling and C(sp^3)-H bond activation. Angew Chem Int Ed Engl 2006; 45: 2289-2292.
[17] Ishiyama T, Murata M and Miyaura N. Palladium(0)-catalyzed cross-coupling reaction of alkoxydiboron with haloarenes: a direct procedure for arylboronic esters. J Org Chem 1995; 60: 7508-7510.
[18] Lin S, Wang C, Ji M, Wu D, Lv Y, Sheng L, Han F, Dong Y, Zhang K, Yang Y, Li Y, Chen X and Xu H. Discovery of new thienopyrimidine derivatives as potent and orally efficacious phosphoinositide 3-kinase inhibitors. Bioorg Med Chem 2018; 26: 637-646.
[19] Wang X, Xu W, Miao C, Dong F, Li W, Wang M, Gao M, Zheng QH and Xu Z. Synthesis of *N*-(3-(4-[^{11}C]methylpiperazin-1-yl)-1-(5-methylpyridin-2-yl)-1*H*-pyrazol-5-yl)pyrazolo[1,5-*a*]pyrimidine-3-carboxamide as a new potential PET agent for imaging of IRAK4 enzyme in neuroinflammation. Appl Radiat Isot 2018; 132: 6-12.
[20] Dong F, Du J, Miao C, Jia L, Li W, Wang M, Zheng QH and Xu Z. Radiosynthesis of carbon-11 labeled PDE5 inhibitors as new potential PET radiotracers for imaging of Alzheimer's disease. Appl Radiat Isot 2019; 154: 108873.
[21] Gao M, Wang M and Zheng QH. Synthesis of carbon-11-labeled CK1 inhibitors as new potential PET radiotracers for imaging of Alzheimer's disease. Bioorg Med Chem Lett 2018; 28: 2234-2238.
[22] Jewett DM. A simple synthesis of [^{11}C]methyl triflate. Int J Rad Appl Instrum A 1992; 43: 1383-1385.
[23] Xu Z, Jia L, Liu W, Li W, Song Y and Zheng QH. Radiosynthesis of a carbon-11 labeled PDE5 inhibitor [^{11}C]TPN171 as a new potential PET heart imaging agent. Appl Radiat Isot 2020; 162: 109190.
[24] Wang M, Gao M, Miller KD and Zheng QH. Synthesis of [^{11}C]PBR06 and [^{18}F]PBR06 as agents for positron emission tomographic (PET) imaging of the translocator protein (TSPO). Steroids 2011; 76: 1331-1340.
[25] Mock B, Glick-Wilson BE, Zheng QH and Degrado T. Automated measurement of specific activity of radiolabeled ligands during synthesis. J Labelled Compd Radiopharm 2005; 48: S224.
[26] Mock BH, Zheng QH and DeGrado TR. A multipurpose ^{11}C-radio-synthesis system. J Labelled Compd Radiopharm 2005; 48: S225.
[27] Wang M, Gao M and Zheng QH. Fully automated synthesis of PET TSPO radioligands [^{11}C]DAA1106 and [^{18}F]FEDAA1106. Appl Radiat Isot 2012; 70: 965-973.
[28] Zheng QH and Mock BH. Purification of carbon-11 PET radiotracers from unlabeled precursors by preparative HPLC and SPE. Biomed Chromatogr 2005; 19: 671-676.
[29] Wang M, Glick-Wilson BE and Zheng QH. Fully automated radiosynthesis and quality control of estrogen receptor targeting radiopharmaceutical 16α-[^{18}F]fluoroestradiol ([^{18}F]FES) for human breast cancer imaging. Appl Radiat Isot 2020; 160: 109109.